Available Online at http://www.jart.ma

Journal of Atlantic Research and Technology

Hydrous Niobium Oxide $Nb_2O_5.xH_2O$ as a Natural Adsorbent for Methylene Blue: Mechanistic and Isotherm Insights.

Abduraboh Alraae[a], Asmaa Mourhly[a], Ely Cheikh Moine[b], Soukaina Belekbir[a], Aicha Sifou[a], Mohammed Dahhou[a], Mouatamid El Hazzat[a,*]

[a] *Laboratory of Materials, Nanotechnologies and Environment, Faculty of Sciences, Mohammed V University in Rabat, Morocco.*

[b] *Membranes, Materials, Environment, and Aqueous Medium, University of Nouakchott, Mauritania*

ARTICLE INFO

Article history:
Received 2nd February 2025
Received in revised form 15h April 2025
Accepted 20th April 2025
Available online 30th April, 2025

Keywords:
Niobium oxide
Methylene blue
Adsorption
Kinetic studies
Isotherm

ABSTRACT

In this study, the adsorption of methylene blue dye (MB) on hydrous niobium oxide, a natural product present in Brazil, was examined in a batch system. The material was characterized via X-ray diffraction (XRD), Fourier transform infrared (FTIR), and thermogravimetry (TG). The ability of $Nb_2O_5.xH_2O$ to adsorb MB was examined at room temperature by varying different parameters, such as pH, adsorbent dose, contact time, and initial concentration. The optimum adsorption was obtained at pH 5 and a solid/solution ratio of 4. The adsorption efficiency, obtained after 40 and 150 min of contact, was evaluated to be 70% and 65% at initial concentrations of 50 and 80 mg/L, respectively. Kinetics modelling revealed that MB removal is a multistep mechanism that begins with external diffusion of the pollutant through the solution to the external surface of the solid, followed by intraparticle diffusion and, finally, surface reactions. The latter was found following the pseudo-first-order and pseudo-second-order adsorption models at low and high MB concentrations, respectively, which was probably related to the agglomeration phenomenon of MB dye molecules at high concentrations. According to the adsorption isotherm modelling, the Freundlich and Sips models were found to better describe the equilibrium state, with a maximum capacity of 87.6 mg/g.

1. Introduction

Water is a valuable resource for all living organisms, even though its pollution by organic and inorganic compounds has become a serious public concern. The main sources of freshwater pollution are industrial effluents and wastes [1,2], which are considered toxic to aquatic life and are responsible for more than 70–80% of human diseases in developing countries [3]. The presence of colored organic pollutants in water presents a high contamination risk for aquatic organisms because they prevent the penetration of sunlight and consume water oxygen when degrading, which increases the demand for biological oxygen [4]. Dyes are colored organic compounds released by the textile, paper, food and other industries. Even at low concentrations, they can have significant undesirable effects on the hydrosphere due to their recalcitrant nature, as well as their carcinogenic, mutagenic, or teratogenic nature [5,6].

The removal of dyes from aqueous solutions has been performed via different methods, such as membrane separation [7], adsorption [8], and photocatalytic degradation [9]. The removal of these compounds via adsorption processes on different solid materials has been the subject of several studies [4]. Adsorption on activated carbon was found to be a highly efficient processing technique [10]. However, in the case of certain recalcitrant dyes, coal overdoses are needed for better treatment, which results in excessive operation costs. To replace activated carbon, many researchers have focused, in recent years, on the preparation of low-cost solid adsorbents that require little processing and are abundant in nature, such as clays, zeolites, and biomass, or are generated from industry, such as byproducts and waste materials [11]. These nonconventional low-cost adsorbents, which are available at very low prices, have proven their efficiency for the removal of MB dye [11].

*Corresponding author.

E-mail address: mouatamid.elhazzat@gmail.com

Hydrous niobium oxide, a natural product available in Brazil with the largest deposit (85% of the world supply) [12], has many remarkable properties and is used in a wide range of applications. It is mainly used as a support in acid-catalyzed reactions because of its strong surface acidity and stability in aqueous media [13]. Indeed, niobium oxides have been used in ethylene hydration [14], esterification of vegetable oils [15], dehydration of alcohols [16], condensation of halochromic compounds [17], and epoxidation of methyl oleate [18]. It is also used in the photodegradation of organic pollutants [19], as an adsorbent for the removal of phosphate ions, H_2 and H_2S [20,21], or as a carrier in biomass immobilization [22]. In the present study, we evaluated the ability of hydrous niobium oxide to adsorb methylene blue dye (MB) from aqueous solution through kinetics and isotherm modelling.

2. Materials and Methods

2.1. *Materials*

The sorbent material hydrous niobium oxide $Nb_2O_5.nH_2O$ was supplied by Companhia Brasileira de Metalirgia e Mineracao (CBMM) and was used without prior treatment. Methylene blue dye was obtained from Sigma–Aldrich Chemicals. The structure of methylene blue and its main properties are summarized in Table 1. The solution pH was adjusted by using either 0.1 M HCl or NaOH.

Table 1
Main properties of methylene blue dye

Name	Methylene blue
Molecular formula	$C_{16}H_{18}N_3SCl$
Molecular weight (g/mol)	319.85
Purity (%)	≤85
Maximum wavelength (nm)	668
Chemical structure	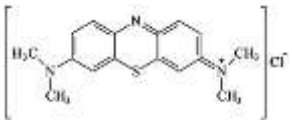

2.2. *Characterization*

XRD analysis was carried out to identify and assess the phase purity obtained after different calcinations. The diagrams were collected via a Siemens D500 Powder Diffractometer equipped with a copper anticathode ($\lambda_{CuK\alpha}$=1.541838 Å) at a scanning speed of 0.02° s^{-1}. FTIR-ATR characterization of the samples was performed via a Jasco FT/IR 4600 spectrometer equipped with a Jasco ATR PRO ONE module. The samples were scanned in transmission mode with 4 cm^{-1} resolution in the range of 4000–400 cm^{-1}. TEM–EDS micrographs were obtained with a Tecnai G2 instrument (FEI company) operating at 120 kV with 0.35 nm resolution and equipped with an EDS microanalyzer. The simultaneous TG/DTG/DTA analyses were carried out on a Labsys^{TM} Evo (1F) Setaram apparatus.
The residual MB concentration in the solution was measured via a UV–Vis spectrophotometer (UV2300) at a maximum wavelength of 668 nm. The solution pH values were measured with a Hanna pH-211R pH meter equipped with an electrode of glass combined with HI1131B.

2.3. *Surface charge characterization*

The point of zero charge is an important parameter that characterizes the surface of materials since it indicates the pH at which the sorbent has a zero-surface charge. The determination of the pH_{PZC} was carried out as follows: different batch systems were prepared containing 50 ml NaCl (0.01 M). The solution pH was then adjusted to values between 2 and 12 by adding either HCl or NaOH (0.1 M) solutions. A mass of 0.15 g of the sample was then added, and the mixture was agitated for 48 h at room temperature. The final pH was measured. The point of zero charge is the point where the curve pH_f vs. pH_i crosses the diagonal line.

2.4. *Sorption experiments*

All the sorption experiments were conducted via a batch technique at room temperature. A series of 50 ml MB solutions with concentrations of 50 and 80 mg/l were put in contact with a given mass of hydrous niobium oxide. The mixture was shaken on a mechanical shaker set at 300 rpm at different time intervals. The initial solution pH was adjusted to the desired level before adding the sorbent. For the equilibrium isotherm experiments, 0.2 g of the sorbent was mixed with 50 ml of MB solutions of different initial concentrations ranging from 40 to 90 mg/l at a stirring speed of 300 rpm until the equilibrium time was reached.

3. Results and discussion

3.1. Characterization

The X-ray powder diffraction pattern of the hydrous niobium oxide is shown in Figure 1a. The strong broad humps between 19 and 39° (2θ) and between 39 and 70° (2θ) indicate that the sample is amorphous and has no crystalline structure, as described in the literature [23,24]. The extensive peak broadening indicates the ultrafine dimension of the particles. The FTIR spectrum of the investigated sample is displayed in Figure 1.b. The bands observed at 3000 and 1625 cm-1 correspond to water and hydroxyl groups. The bands at 930 and 660 cm-1 and the shoulder at 585 cm-1 correspond to the Nb-O stretching vibrations of highly distorted and slightly distorted NbO6 octahedra, respectively. These results are typical of those reported in the literature [23].

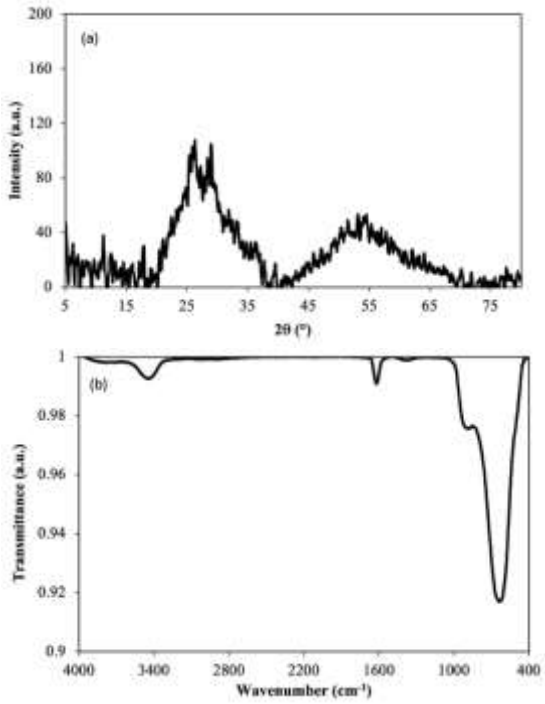

Fig. 1. X-ray diffraction and FTIR-ATR spectra of hydrous NO

Figure 2 shows the results of simultaneous TG/DTG/DTA thermal analysis of hydrous niobium oxide at a heating rate of 10°C/min under an air atmosphere with a flow rate of 60 ml/min. The TG thermogram revealed continuous mass loss from ambient temperature to 270°C, which was associated with complex endothermic overlapping peaks observed via DTA. This mass loss can be attributed to the dehydration of the sample [15]. The sharp exothermic peak observed with no mass loss at 571.96°C corresponds to the crystallization of niobium oxide Nb2O5 [25].

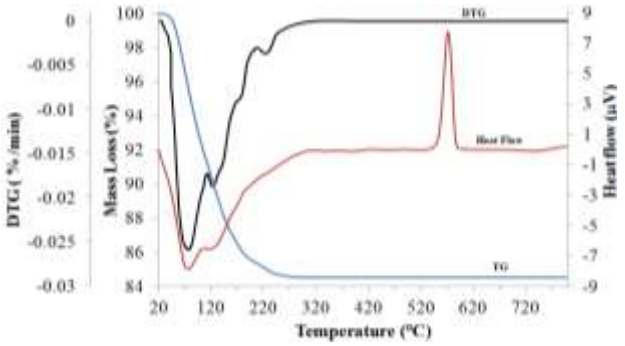

Fig. 2. Analysis of hydrous niobium oxide via a simultaneous TG/DTG/DTA apparatus

3.2. Adsorption of MB on hydrous niobium oxides

3.2.1. Effect of solution pH

pH is an important parameter during the sorption process because it affects both the solute and surface properties of the sorbent. In accordance with the work of Wesolowski et al. [26], the solution pH changes the structure and dynamics of both the aqueous and solid phases and induces the sorption of anions and cations dissolved in the solution. Thus, depending on the solution pH, the surface of a material can be dominated by positive charges or negative charges. The pH at which the solid surface has equal concentrations of negatively and positively charged sites is called the point of zero charge (pH_{PZC}).

The pH_{PZC} of hydrous niobium oxide was examined at ambient temperature by placing 50 cm^3 of 0.01 M NaCl solution in a volumetric flask. The pH was then adjusted to values ranging from 2 to 12 with 0.1 M NaOH or HCl. A mass of 0.15 g of hydrous niobium oxide was subsequently added to the solution, and the final pH was measured after 48 h under stirring. pH_{PZC} is the value where the curve of pH_f vs. pH_i meets the diagonal line (Figure 3). The found value is approximately 3.5, which is near the value reported in earlier studies [20]. Thus, at a lower pH (<3.5), the adsorbent surface is positively charged and can carry negative ions. On the other hand, when the solution pH increases, the surface becomes more negatively charged and attracts more cationic ions.

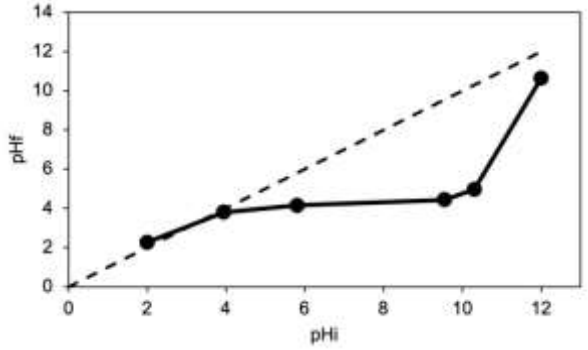

Fig. 3. Point of zero charge determination of hydrous niobium oxide

To evaluate the effect of the solution pH on adsorption, 50 ml of MB solution at an initial concentration of 50 mg/l was mixed with 4 g/l adsorbent. The initial solution pH was varied between 2 and 11, and the mixture was stirred at 300 rpm for 300 min (Figure 4). The percentage of MB removed from hydrous niobium oxide increased with increasing solution pH and reached a maximum value at pH values equal to or above 5, which is in accordance with the pHPZC results. This finding indicates that the adsorption of MB is strongly dependent on the solution pH [20]. Thus, for further study, the optimal pH of 5 was used.

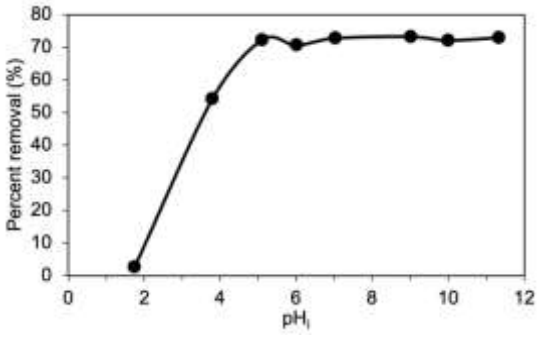

Fig. 4. Effects of solution pH on the adsorption of MB on hydrous niobium oxide

3.2.2. *Effect of the solid/solution ratio*

The effect of the solid/solution ratio was investigated by varying either the adsorbent mass or the solution volume. In the first case, different amounts of adsorbent, ranging from 0.05 to 0.4 g, were added to 50 mL of MB solution at a concentration of 50 mg/L. The mixtures were shaken for 60 minutes at 180 rpm. In the second case, the solution volume was varied by adding 0.2 g of adsorbent to MB solutions (50 mg/L) with volumes ranging from 30 to 200 mL. The effect of the solid-to-solution ratio on the adsorption of MB onto hydrous niobium oxide is presented in Figure 5.

According to the obtained results, increasing the solid/solution ratio increased the percentage of MB removed (Figure 5b) but decreased the equilibrium adsorbed quantity, Qe (Figure 5a). During the variation in solution volume, low values of percent removal and Qe are observed at a volume of 200 ml, which is most likely due to the large separation distance between the active sites of the adsorbent and the MB particles. The increase in percent removal at ratios above 2 may be explained by the increase in the number of sites available per unit volume of MB solution. An almost constant shape is observed above a ratio of 4, which promotes the optimal value for the adsorption process of MB on hydrous niobium oxide.

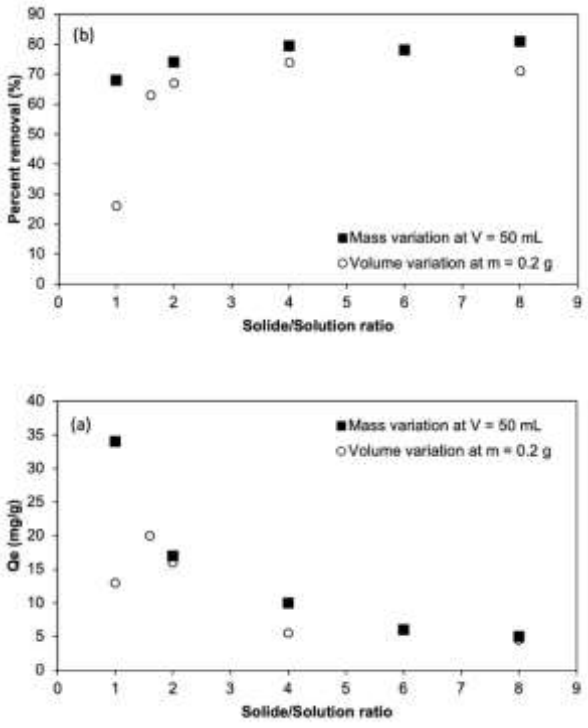

Fig. 5. Effects of the solid/solution ratio on the adsorption of MB on hydrous niobium oxide

3.2.3. Effects of the contact time and initial concentration

The effects of contact time and initial concentration on the adsorption process were studied by shaking a series of suspensions containing 0.2 g of hydrous niobium oxide and 50 or 80 mg/l MB solutions adjusted to pH 5. The amount adsorbed was measured at different time intervals ranging from 5--300 min, as shown in Figure 6.

The results showed that the adsorption process was very fast during the first 15 min before gradually reaching equilibrium. After 40 and 150 min, the removal efficiency was evaluated to be approximately 70% and 65% for initial MB dye concentrations of 50 and 80 mg/L, respectively. The first high adsorption speed is due to the large number of sorption sites available on the solid surface [27]. The observed decrease in the percent removal when the initial concentration of MB dye was increased is probably due to the limited number of active sites available. However, the adsorbed amount (Qe) increased from 9.20 to 13.19 mg/g when the initial concentration of MB increased, which was related to the driving force needed to overcome the resistance of mass transfer between the liquid and solid phases [28].

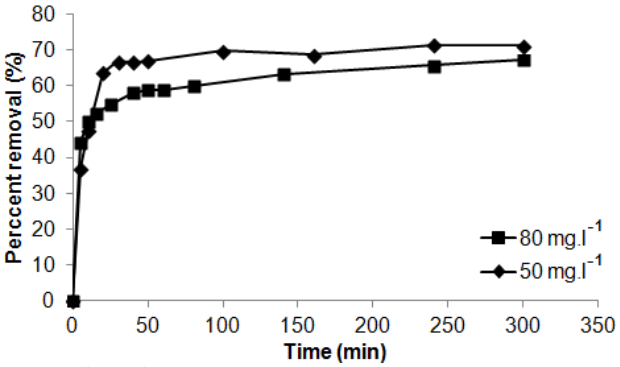

Fig. 6. Effects of contact time and initial concentration on the adsorption of MB on hydrous niobium oxide

The results showed that the adsorption process was very fast during the first 15 min before gradually reaching equilibrium. After 40 and 150 min, the removal efficiency was evaluated to be approximately 70% and 65% for initial MB dye concentrations of 50 and 80 mg/L, respectively. The first high adsorption speed is due to the large number of sorption sites available on the solid surface [27]. The observed decrease in the percent removal when the initial concentration of MB dye was increased is probably due to the limited number of active sites available. However, the adsorbed amount (Qe) increased from 9.20 to 13.19 mg/g when the initial concentration of MB increased, which was related to the driving force needed to overcome the resistance of mass transfer between the liquid and solid phases [28].

3.3. *Kinetic study*

3.3.1. *External and intraparticle diffusion*

The role of external diffusion in the adsorption process of MB dye on hydrous niobium oxide was evaluated via the mathematical model proposed by Furusawa and Smith [29] and Mckay [30]:

$$\frac{C_t}{C_0} = \frac{1}{1+m_s K_L} + B \times \exp\left[-\frac{k_f \times S_S \times t}{B}\right] \quad (1)$$

where C0 is the initial concentration of solute (mg/l), B is a constant equal to $\frac{m_S K_L}{1+m_S K_L}$, ms is the sorbent concentration (g/l), K_L is the Langmuir constant (l/g), Ss is the surface area of the sorbent (m^2/l), and k_f is the coefficient of external mass transfer.

Nonlinear regression was used to evaluate the goodness of fit of the model and the equation parameters.

The intraparticle diffusion step can be modelled via the Weber and Morris equation [31], expressed as follows:

$$q_t = k_{dif}.t^{1/2} + C \qquad (2)$$

where q_t is the quantity adsorbed at time t (mg/g), kdif is the constant diffusion rate (mg/g min^{-1}), and C is the double-layer thickness (mg/g).

The plot of the adsorption capacity q_t vs. the square root of time $t_{1/2}$ must be a straight line if intraparticle diffusion is a controlling factor during the adsorption process. The plot can also yield multiple lines indicating the occurrence of different steps during the removal process [32,33].

The obtained plots of equations (1) and (2) are shown in Figures 7a and 7b, respectively, and the deduced kinetic parameters are listed in Table 2.

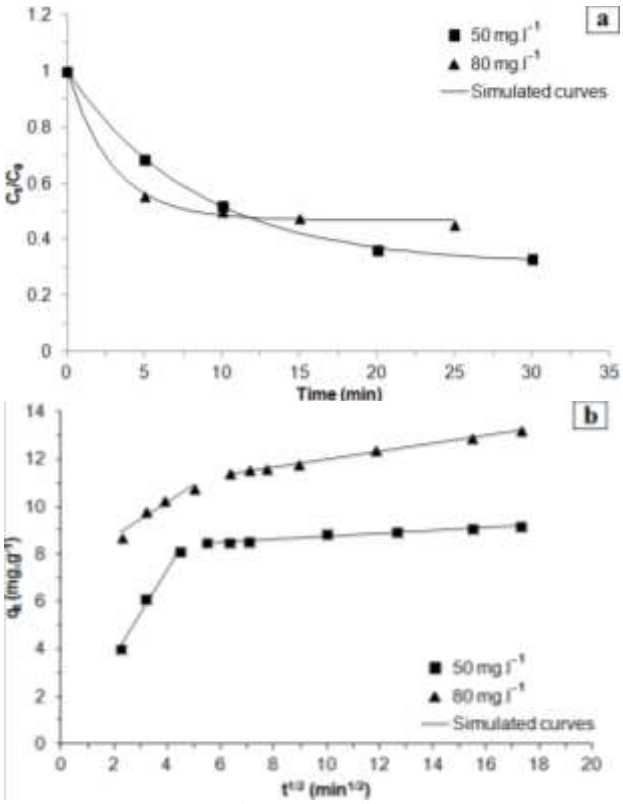

Fig. 7. Kinetic modelling of a) external diffusion and b) intraparticle diffusion processes

The results shown in Figure 8a indicate good correlation of the external diffusion model with the experimental data during the first adsorption minutes for both concentrations. On the other hand, the intraparticle diffusion modelling results in Figure 7b indicate the presence of two straight lines. According to previous works, these lines indicate the existence of a multistep mechanism during the adsorption process [27,32,34]. The initial sharper portion corresponds to the external diffusion of MB dye through the solution to the external surface of the adsorbent, and the second stage is the region where intraparticle diffusion predominates. The intercept obtained from extrapolating the linear portion of the plots to the Y-axis provided an ideal thickness of boundary layer C and indicated the presence of boundary layer resistance at the early stage of adsorption. When the initial MB concentration increased, the rate parameters of external mass diffusion kf and intraparticle diffusion kdif increased, as shown in Table 2. This increase is due to the increase in the driving force, as we can conclude from Fick's first law of diffusion [35].

Table 2

Kinetic parameters of the external and intraparticle diffusion models

External diffusion			
C_i (mg/l)	**K_L (l/g)**	**$k_f S_s$ (min^{-1})**	**R^2**
50	0,5623	0,0827	0.9994
80	0,2837	0,1833	0.9987
Intraparticle diffusion			
C_i (mg/l)	**k_{dif} ($mg.g^{-1}.min^{-1/2}$)**	**C (mg/g)**	**R^2**
50	0.063	8.312	0.966
80	0.165	10.349	0.995

3.3.2. Surface reaction

The commonly used surface adsorption models are the pseudo-first order, pseudo-second order, and Elovich models. The corresponding equations are listed in Table 3.

Table 3

Reaction models used for surface reaction modelling

Pseudo-first order	Pseudo-second order	Elovich
$q_t = q_e(1-\exp(-k_1 t))$	$q_t = \frac{q_e^2 k_2 t}{1+q_e k_2 t}$	$q_t = \frac{1}{b_E}.\ln(1+a_E.b_E.t)$

where qt is the amount adsorbed at time t, qe is the amount adsorbed at equilibrium, k1 is the pseudo-first-order kinetic constant (min^{-1}), k_2 is the pseudo-second-order kinetic constant ($g.mg^{-1}.min^{-1}$), aE is a constant related to the chemisorption rate ($mg.min^{-1}.g^{-1}$), and b_E is a constant related to the rate of surface recovery ($g.mg^{-1}$).

Nonlinear regression was used to evaluate the appropriate model for describing the adsorption process of MB dye on hydrous niobium oxide. The obtained fitted curves and parameters are displayed in Figure 8 and Table 4, respectively.

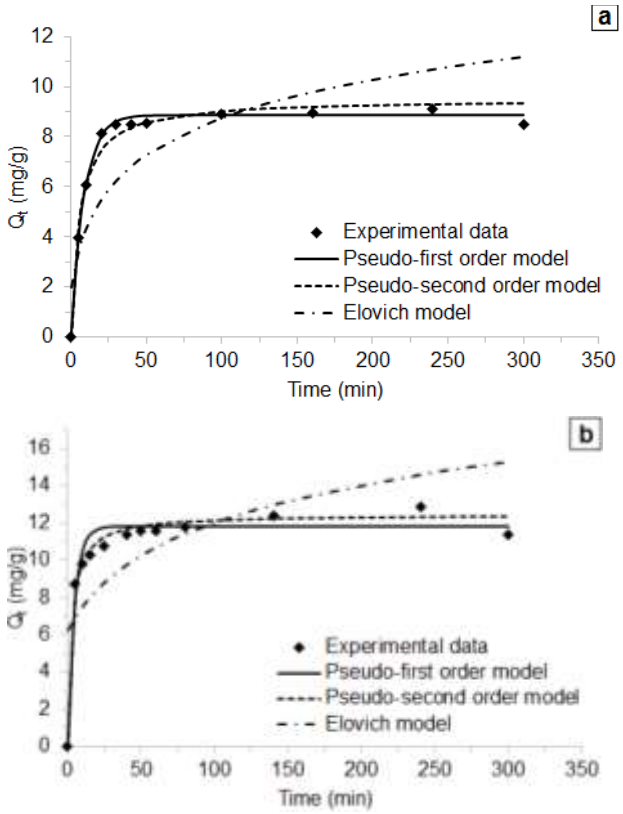

Fig. 8. Kinetic modelling of MB dye adsorption on hydrous niobiom oxide: a) 50 mg.L^{-1} and b) 80 mg.L^{-1}

Table 4
Kinetic parameters of the adsorption of MB dye on hydrous niobium oxide

	Pseudo-first order model			Pseudo-second order model			Elovich model		
$Q_{e,exp}$ (mg.g^{-1})	K_1 (min^{-1})	q_e (mg.g^{-1})	SSE	K_2 (g.mg^{-1}.min^{-1})	q_e (mg.g^{-1})	SSE	a_e (mg.min^{-1}.g^{-1})	b_e (g.mg^{-1})	SSE
50	0.117	8.870	0.375	0.019	9.492	1.100	1.414	0.439	30.342
80	0.216	11.820	7.131	0.030	12.466	2.111	5.428	0.299	69.040

mechanism may be due to the agglomeration of dye molecules at high concentrations, which may decrease the preferential adsorption of MB and thus increase the equilibrium time [36].

3.4. Isotherm study

The effect of initial concentration on MB dye adsorption by hydrous niobium oxide was examined via three isotherm models, namely, the Langmuir, Freundlich, and Sips models (Table 5).

Table 5
Most commonly used isotherm models

Langmuir [37]	Freundlich [38]	Sips [39]
$Q_e = \frac{Q_{max} K_L Ce}{1 + K_L Ce}$	$Q_e = K_F C_e^{1/n_F}$	$Q_e = \frac{Q_{max} (a_S C_e)^{n_S}}{1 + (a_S C_e)^{n_S}}$

Where Qe is the amount adsorbed at equilibrium (mg.g^{-1}), Ce is the concentration of MB dye remaining in solution at equilibrium (mg.l^{-1}), Q_{max} is the maximum capacity of the adsorbent (mg.g^{-1}), K_L is the Langmuir constant (l.mg^{-1}), KF is the Freundlich isotherm constant (mg.l.g^{-1}), and as Sips model constant (l.mg^{-1}), $1/n_f$ is the parameter related to surface heterogeneity, as this parameter is near 0, the surface is more heterogeneous, and n_S is a heterogeneity index.

The parameters calculated via the nonlinear regression method are presented in Table 5, and the fits of the experimental data are shown in Figure 9.

Table 6
Isotherm modelling parameters for the removal of MB dye by hydrous niobium oxide

Langmuir			Freundlich			Sips			
Q_m (mg.g^{-1})	K_L (l.mg^{-1})	SSE	K_F (mg.l.g^{-1})	$1/n_F$	SSE	a_S (l.mg^{-1})	Q_m (mg.g^{-1})	n_S	SSE
22.58	0.033	0.745	1.949	0.507	0.138	0.001	87.60	0.579	0.150

The SSE values obtained for the different models at concentrations of 50 mg.L^{-1} and 80 mg.L^{-1} indicate that the surface reaction step of the adsorption process follows the pseudo-first-order model and pseudo-second-order model, respectively, with an estimated equilibrium capacity similar to the experimental capacity. A comparison of the results obtained from the different diffusion and surface reaction models revealed that the adsorption mechanism of MB by hydrous niobium oxide seems to depend strongly on the dye concentration. This change in the adsorption

The obtained results show that the Freundlich and Sips models better describe the experimental data. Therefore, the adsorption process of MB dye on hydrous niobium oxide follows the Freundlich assumption, which states that multilayer adsorption occurs over a heterogeneous surface. The maximum amount obtained from the Sips model is approximately 87.6 mg/g, which is near the value observed for other metal oxides (Table 7).

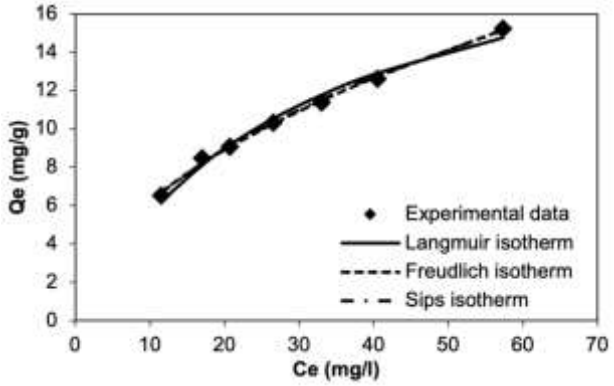

Fig. 9. Isotherm modelling of MB dye adsorption on hydrous niobiom oxide

Table 7
Adsorption capacity of several metal oxides

Materials	Adsorbate	Q_{max} (mg/g)	Reference
TiO_2	Reactive Red 198	86.96	[40]
MgO	Reactive blue 19	166.7	[41]
	Reactive red	123.5	[41]
$FeTiO_3$	Methylene blue	71.9	[42]
Nb_2O_5,xH_2O	Methylene blue	87.6	Present study

4. Conclusion

Hydrous niobium oxide was proven to be effective for the removal of MB dye from aqueous solutions. The effect of the solution pH during the adsorption process was prominent; thus, at pH values above 5, the removal process was at its maximum. The contact time effect, studied at ambient temperature, pH 5, and a solid/solution ratio of 4, resulted in very fast adsorption during the first 15 min, and an efficient removal of approximately 70% was obtained after 40 min of interaction. Adsorption kinetics modelling revealed that the diffusion process predominates throughout the removal process and begins with external diffusion of the adsorbent followed by intraparticle diffusion. Surface adsorption modelling revealed that the surface mechanism strongly depends on the initial MB concentration because of the agglomeration of dyes at high concentrations. Isotherm modelling revealed that the Freundlich and Sips models were the most effective, which indicates that the multilayer adsorption mechanism over a heterogeneous surface has a maximum amount of approximately 87.6 mg/g.

Acknowledgement

The authors thank the staff of the analysis and characterization platform of the Chemistry Department, FSR Rabat, and the National Center of Scientific and Technical Research (CNRST) for their assistance in the experimentation.

Conflicts of interest statement

The authors declare no competing financial interest.

References

[1] K. Ivanov, E. Gruber, W. Schempp, D. Kirov, Possibilities of using zeolite as filler and carrier for dyestuffs in paper, Papier. 50 (1996) 456–459.
[2] I. Kabdasli, O. Tunay, O. D, Wastewater control and management in a leather tanning district, Water Sci. Technol. 40 (1999) 261–267. doi:10.1016/S0273-1223(99)00393-5.
[3] WHO/UNICEF, Global Water Supply and Sanitation Assessment Report 2000, Geneva, 2000.
[4] M.T. Yagub, T.K. Sen, S. Afroze, H.M. Ang, Dye and its removal from aqueous solution by adsorption: a review., Adv. Colloid Interface Sci. 209 (2014) 172–184. doi:10.1016/j.cis.2014.04.002.
[5] M. Oplatowska, R.F. Donnelly, R.J. Majithiya, D. Glenn Kennedy, C.T. Elliott, The potential for human exposure, direct and indirect, to the suspected carcinogenic triphenylmethane dye Brilliant Green from green paper towels., Food Chem. Toxicol. 49 (2011) 1870–6. doi:10.1016/j.fct.2011.05.005.
[6] R.O. Alves de Lima, A.P. Bazo, D.M.F. Salvadori, C.M. Rech, D. de Palma Oliveira, G. de Aragão Umbuzeiro, Mutagenic and carcinogenic potential of a textile azo dye processing plant effluent that impacts a drinking water source, Mutat. Res. - Genet. Toxicol. Environ. Mutagen. 626 (2007) 53–60. doi:10.1016/j.mrgentox.2006.08.002.
[7] S. Zinadini, A.A. Zinatizadeh, M. Rahimi, V. Vatanpour, H. Zangeneh, M. Beygzadeh, Novel high flux antifouling nanofiltration membranes for dye removal containing carboxymethyl chitosan coated Fe_3O_4 nanoparticles, Desalination. 349 (2014) 145–154. doi:10.1016/j.desal.2014.07.007.
[8] M. Rafatullah, O. Sulaiman, R. Hashim, A. Ahmad, Adsorption of methylene blue on low-cost adsorbents: A review, J. Hazard. Mater. 177 (2010) 70–80. doi:10.1016/j.jhazmat.2009.12.047.
[9] M.L. Yola, T. Eren, N. Atar, S. Wang, Adsorptive and photocatalytic removal of reactive dyes by silver nanoparticle-colemanite ore waste, Chem. Eng. J. 242 (2014) 333–340. doi:10.1016/j.cej.2013.12.086.
[10] G. Mezohegyi, F.P. van der Zee, J. Font, A. Fortuny, A. Fabregat, Towards advanced aqueous dye removal processes: A short review on the versatile role of activated carbon, J. Environ. Manage. 102 (2012) 148–164. doi:10.1016/j.jenvman.2012.02.021.
[11] G. Crini, Nonconventional low-cost adsorbents for dye removal: A review, Bioresour. Technol. 97 (2006) 1061–1085. doi:10.1016/j.biortech.2005.05.001.
[12] P.F. de O. Cordeiro, J.A. Brod, M. Palmieri, C.G. de Oliveira, E.S.R. Barbosa, R.V. Santos, et al., The Catalão I niobium deposit, central Brazil: Resources, geology and pyrochlore chemistry, Ore Geol. Rev. 41 (2011) 112–121. doi:10.1016/j.oregeorev.2011.06.013.
[13] Y. Zhao, X. Zhou, L. Ye, S.C. Edman, Nanostructured Nb_2O_5 catalysts, Nano Rev. 3 (2012) 17631–17641. doi:10.3401/nano.v3iO.17631.
[14] Y. Li, S. Yan, B. Yue, W. Yang, Z. Xie, Q. Chen, et al., Selective catalytic hydration of ethylene oxide over niobium oxide supported on α-alumina, Appl. Catal. A Gen. 272 (2004) 305–310. doi:10.1016/j.apcata.2004.06.001.
[15] R.F. Brandão, R.L. Quirino, V.M. Mello, A.P. Tavares, A.C. Peres, F. Guinhos, et al., Synthesis, characterization and use of Nb_2O_5 based catalysts in producing biofuels by transesterification, esterification and pyrolysis, J. Braz. Chem. Soc. 20 (2009) 954–966. doi:10.1590/S0103-50532009000500022.
[16] M.J.C. Molina, M.L. Granados, A. Gervasini, P. Carniti, Exploitment of niobium oxide effective acidity for xylose dehydration to furfural, Catal. Today. 254 (2015) 90–98. doi:10.1016/j.cattod.2015.01.018.
[17] S. Impellizzeri, S. Simoncelli, C. Fasciani, M. Luisa Marin, G.L. Hallett-Tapley, G.K. Hodgson, et al., Mechanistic insights into the Nb_2O_5 and niobium phosphate catalyzed in situ condensation of a fluorescent halochromic assembly, Catal. Sci. Technol. 5 (2015) 169–175. doi:10.1039/C4CY00703D.
[18] R. Turco, A. Aronne, P. Carniti, A. Gervasini, L. Minieri, P. Pernice, et al., Influence of preparation methods and structure of niobium oxide-based catalysts in the epoxidation reaction, Catal. Today. 254 (2015) 99–103. doi:10.1016/j.cattod.2014.11.033.

[19] A.G.S. Prado, L.B. Bolzon, C.P. Pedroso, A.O. Moura, L.L. Costa, Nb2O5 as efficient and recyclable photocatalyst for indigo carmine degradation, Appl. Catal. B Environ. 82 (2008) 219–224. doi:10.1016/j.apcatb.2008.01.024.
[20] L.A. Rodrigues, M.L.C.P. da Silva, Thermodynamic and kinetic investigations of phosphate adsorption onto hydrous niobium oxide prepared by homogeneous solution method, Desalination. 263 (2010) 29–35. doi:10.1016/j.desal.2010.06.030.
[21] E. Ozdogan, J. Wilcox, Investigation of H_2 and H_2S adsorption on niobium- and copper-doped palladium surfaces., J. Phys. Chem. B. 114 (2010) 12851–12858. doi:10.1021/jp105469c.
[22] M. Miranda, M.L.C. da Silva, H.F. de Castro, Optimized immobilization of microbial lipase on hydrous niobium oxide, J. Chem. Technol. Biotechnol. 81 (2006) 566–572. doi:10.1002/jctb.1474.
[23] I. AL. Bassan, D.R. Nascimento, R. a S. San Gil, M.I.P. Da Silva, C.R. Moreira, W. a. Gonzalez, et al., Esterification of fatty acids with alcohols over niobium phosphate, Fuel Process. Technol. 106 (2013) 619–624. doi:10.1016/j.fuproc.2012.09.054.
[24] L.A. Rodrigues, M.L.C.P. da Silva, Synthesis of $Nb_2O_5{\cdot}nH_2O$ nanoparticles by water-in-oil microemulsion, J. Non. Cryst. Solids. 356 (2010) 125–128. doi:10.1016/j.jnoncrysol.2009.11.002.
[25] A. V. Rosario, E.C. Pereira, Influence of the crystallinity on the Li+ intercalation process in Nb_2O_5 films, J. Solid State Electrochem. 9 (2005) 665–673. doi:10.1007/s10008-004-0637-3.
[26] D.J. Wesolowski, M.L. Machesky, M.K. Ridley, D.A. Palmer, Z. Zhang, P.A. Fenter, et al., Ion Adsorption on Metal Oxide Surfaces to Hydrothermal Conditions., ECS Trans. 11 (2008) 167–180. doi:10.1149/1.2939086.
[27] A. El Hamidi, R. Mulongo Masamba, M. Khachani, M. Halim, S. Arsalane, Kinetics modelling in liquid phase sorption of copper ions on brushite di-calcium phosphate di-hydrate $CaHPO_4{\cdot}2H_2O$ (DCPD), Desalin. Water Treat. 56 (2015) 779–791. doi:10.1080/19443994.2014.940391.
[28] W.-T. Tsai, H.-C. Hsu, T.-Y. Su, K.-Y. Lin, C.-M. Lin, T.-H. Dai, The adsorption of cationic dye from aqueous solution onto acid-activated andesite., J. Hazard. Mater. 147 (2007) 1056–1062. doi:10.1016/j.jhazmat.2007.01.141.
[29] T. Furusawa, J.M. Smith, Fluid-Particle and Intraparticle Mass Transport Rates in Slurries, Ind. Eng. Chem. Fundam. 12 (1973) 197–203. doi:10.1021/i160046a009.
[30] G. Mckay, The adsorption of dyestuffs from aqueous solutions using activated carbon. iv. external mass transfer processes, J. Chem. Technol. Biotechnol. Chem. Technol. 33 (2007) 205–218. doi:10.1002/jctb.504330407.
[31] W. Weber, J. Morris, Kinetics of adsorption on carbon from solution, J. Sanit. Eng. Div. 89 (1963) 31–60.
[32] P. Waranusantigul, P. Pokethitiyook, M. Kruatrachue, E.S. Upatham, Kinetics of basic dye (methylene blue) biosorption by giant duckweed (Spirodela polyrrhiza), Environ. Pollut. 125 (2003) 385–392. doi:10.1016/S0269-7491(03)00107-6.
[33] A.E. Ofomaja, Biosorption studies of Cu(II) onto Mansonia sawdust: Process design to minimize biosorbent dose and contact time, React. Funct. Polym. 70 (2010) 879–889. doi:10.1016/j.reactfunctpolym.2010.08.002.
[34] A.E. Ofomaja, Intraparticle diffusion process for lead(II) biosorption onto mansonia wood sawdust., Bioresour. Technol. 101 (2010) 5868–5876. doi:10.1016/j.biortech.2010.03.033.
[35] P. Marin, C.E. Borba, A.N. Módenes, F.R. Espinoza-Quiñones, S.P.D. de Oliveira, A.D. Kroumov, Determination of the mass transfer limiting step of dye adsorption onto commercial adsorbent by using mathematical models, Environ. Technol. 35 (2014) 2356–2364. doi:10.1080/09593330.2014.904445.
[36] T.S. Natarajan, H.C. Bajaj, R.J. Tayade, Preferential adsorption behavior of methylene blue dye onto surface hydroxyl group enriched TiO2 nanotube and its photocatalytic regeneration, J. Colloid Interface Sci. 433 (2014) 104–114. doi:10.1016/j.jcis.2014.07.019.
[37] I. Langmuir, The adsorption of gases on plane surfaces of glass, mica and platinum, J. Am. Chem. Soc. 40 (1918) 1361–1403. doi:10.1021/ja02242a004.
[38] H.M.F. Freundlich, Over the adsorption in solution, J. Phys. Chem. 57 (1906) 385 – 470.
[39] R. Sips, Combined form of Langmuir and Freundlich equation, J. Phys. Chem. 16 (1948) 490–495.
[40] V. Belessi, G. Romanos, N. Boukos, D. Lambropoulou, C. Trapalis, Removal of Reactive Red 195 from aqueous solutions by adsorption on the surface of TiO2 nanoparticles, J. Hazard. Mater. 170 (2009) 836–844. doi:10.1016/j.jhazmat.2009.05.045.
[41] G. Moussavi, M. Mahmoudi, Removal of azo and anthraquinone reactive dyes from industrial wastewaters using MgO nanoparticles, J. Hazard. Mater. 168 (2009) 806–812. doi:10.1016/j.jhazmat.2009.02.097.
[42] Y.H. Chen, Synthesis, characterization and dye adsorption of ilmenite nanoparticles, J. Non. Cryst. Solids. 357 (2011) 136–139. doi:10.1016/j.jnoncrysol.2010.09.070.